

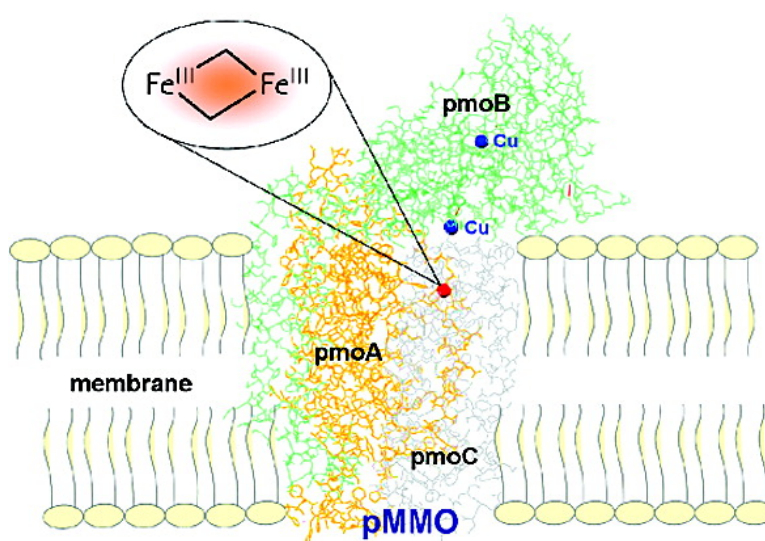
Communication

Mössbauer Studies of the Membrane-Associated Methane Monooxygenase from *Methylococcus capsulatus* Bath: Evidence for a Diiron Center

Marlene Martinho, Dong W. Choi, Alan A. DiSpirito, William E. Antholine, Jeremy D. Semrau, and Eckard Mnck

J. Am. Chem. Soc., **2007**, 129 (51), 15783-15785 • DOI: 10.1021/ja077682b

Downloaded from <http://pubs.acs.org> on February 9, 2009



More About This Article

Additional resources and features associated with this article are available within the HTML version:

- Supporting Information
- Links to the 10 articles that cite this article, as of the time of this article download
- Access to high resolution figures
- Links to articles and content related to this article
- Copyright permission to reproduce figures and/or text from this article

[View the Full Text HTML](#)

Mössbauer Studies of the Membrane-Associated Methane Monooxygenase from *Methylococcus capsulatus* Bath: Evidence for a Diiron Center

Marlène Martinho,[†] Dong W. Choi,[‡] Alan A. DiSpirito,[‡] William E. Antholine,[§]
Jeremy D. Semrau,[¶] and Eckard Münck^{*†}

Department of Chemistry, Carnegie Mellon University, Pittsburgh, Pennsylvania 15213, Department of Biochemistry, Biophysics and Molecular Biology, Iowa State University, Ames, Iowa 50011-3211, Department of Biophysics, Medical College of Wisconsin, Milwaukee, Wisconsin 53226, and Department of Civil and Environmental Engineering, University of Michigan, Ann Arbor, Michigan 48109-2125

Received October 5, 2007; E-mail: emunck@cmu.edu

Methane monooxygenase (MMO) catalyzes the energy-dependent oxidation of methane to methanol in methanotrophic bacteria.^{1,2} In these organisms, two different methane monooxygenases have been identified, namely, a membrane-associated or particulate MMO (pMMO) and a cytoplasmic or soluble MMO (sMMO). In methanotrophs that express both forms of the enzyme, the copper concentration during growth dictates which MMO is expressed.^{2–5} In cells cultured under a low copper/biomass ratio, the sMMO is predominately expressed, whereas cells cultured at higher copper/biomass ratios exclusively express the pMMO (sMMO is not transcribed).^{6–8} The sMMO is a well-characterized three-component enzyme consisting of a hydroxylase, a reductase, and a regulatory protein.^{9–12} Spectroscopic and X-ray crystallographic studies have established that the hydroxylase contains an oxygen-bridged diiron cluster.^{13–16} Here we provide evidence that pMMO contains a diiron cluster as well.

Owing to the low specific activity and instability of most pMMO preparations,^{6,17–20} comparatively little is known about the molecular properties of this enzyme. As isolated, pMMO is composed of three polypeptides with molecular masses of 45 000, 26 000, and 23 000 Da with a subunit structure of ($\alpha\beta\gamma$)₃.^{6,17,18,20–22} Most researchers agree that each $\alpha\beta\gamma$ contains 2–3 Cu atoms,^{2,6,17–20,23} although one group has suggested that 15 Cu atoms are arranged into catalytic and electron-transfer trinuclear copper clusters.^{22,24,25} The 2.8 Å resolution crystal structure of pMMO suggested that each $\alpha\beta\gamma$ contained a dicopper site, a mononuclear copper site, and a third site occupied by zinc.^{21,23} However, the preparation used for growing the crystal was inactive and did not contain zinc (which was added to the crystallization buffer).^{21,23}

The involvement of non-heme iron in methane oxidation by the pMMO has been proposed by some laboratories^{6,17,26–29} and disputed by others.^{22,24,30} In our laboratory at Iowa State University, we have observed that preparations of pMMO showing highest specific activity contain 1–2 iron atoms.⁶ We therefore decided to employ Mössbauer spectroscopy to characterize the iron components. This technique is particularly well-suited to explore iron environments that are EPR-silent and optically uninformative in the visible region, as is the spin-coupled diiron(III) center of the hydroxylation component of sMMO. It seemed reasonable to us to search for a similar diiron cluster because this is the only type of center known to oxidize methane to methanol at room temperature.

The 4.2 K Mössbauer spectrum of the antiferromagnetically coupled diiron(III) centers of sMMO consists of a doublet with quadrupole splitting $\Delta E_Q = 1.12$ mm/s for the *M. capsulatus* Bath

Table 1. Properties of Whole Cells and Purified pMMO Mössbauer Samples

	whole cells	pMMO
$\alpha\beta\gamma$ (mM)	0.56	1.06
total Fe (mM)	5.2	1.2
Fe in doublet 1 (mM)	1.04	0.24
diiron(III)/ $\alpha\beta\gamma$	0.93	0.11
activity (nmol·min ⁻¹ ·mg pMMO protein ⁻¹)	~1500	160

enzyme^{15,31} and $\Delta E_Q = 1.02$ mm/s for that of *M. trichosporium* OB3b;^{13,16} both enzymes have an isomer shift $\delta = 0.50$ mm/s at 4.2 K (the clusters of the two enzymes yield broad absorption lines, and equivalent fits have been obtained by assuming different ΔE_Q values for the two iron sites; see refs 13, 15, 16, and 31).

Table 1 lists analytical and activity data of our purified pMMO sample and of whole cells grown at high copper (80 μ M) and iron (40 μ M); the entries are discussed in the Supporting Information. Figure 1 shows 4.2 K Mössbauer spectra of purified pMMO. The central portion of the 45 mT spectrum (Figure 1A) exhibits two overlapping doublets with $\Delta E_Q(1) = 1.05$ mm/s, $\delta(1) = 0.50$ mm/s (~20% of total Fe), and $\Delta E_Q(2) = 2.65$ mm/s, $\delta(2) = 1.25$ mm/s (~18% of total Fe); the δ value of doublet 2 is characteristic of a high-spin Fe²⁺ with octahedral N/O coordination. The majority of the iron in the spectrum of Figure 1A, perhaps up to 60% of total Fe, belongs to a heterogeneous population of Fe³⁺ species exhibiting magnetic hyperfine structure with splittings up to 17 mm/s Doppler velocity. This Fe³⁺ fraction is EPR-silent at X-band (Figure S3), and its ΔE_Q and δ values (0.63 and 0.51 mm/s at 120 K) are the same as those reported for mineralized nanoparticles (attributed to ferric phosphate) in mitochondria of the yeast frataxin homologue ($\Delta yfh1$) mutants.³² The ΔE_Q and δ values of doublet 1 match those reported for the diiron(III) centers of sMMO. The solid line in Figure 1A is a spectral simulation representing two doublets 1 and 2, drawn such that their sum represents 38% of the total iron; the features of doublet 1 are indicated by the offset dashed line.

The spectrum of Figure 1B was recorded in an applied magnetic field of 8.0 T. Most interestingly, the 8.0 T spectrum shows that the iron of doublet 1 belongs to a diamagnetic ($S = 0$) center, as demonstrated by the spectral simulation outlined by the vertically displaced solid line. The values of $\Delta E_Q(1)$ and $\delta(1)$, together with the observed diamagnetism of this spectral component, strongly suggest that doublet 1 represents an antiferromagnetically coupled diiron(III) center similar to that found in sMMO.

Mössbauer spectroscopy is a very useful technique for the study of iron-containing proteins in whole cells, provided the concentration of the targeted proteins can be increased by overexpression³³ or by employing special growth conditions. Since *M. capsulatus* Bath produces large amounts of pMMO (~20% of whole cell

[†] Carnegie Mellon University.

[‡] Iowa State University.

[§] Medical College of Wisconsin.

[¶] University of Michigan.

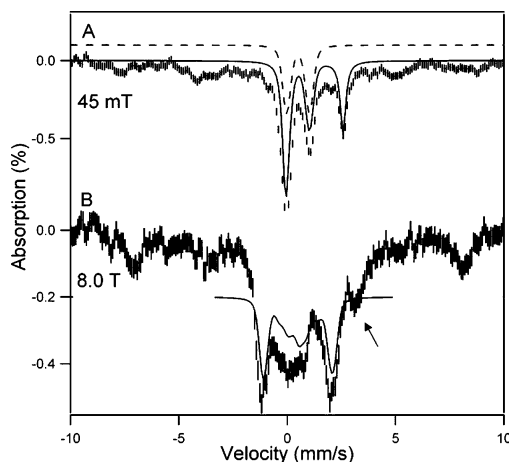


Figure 1. 4.2 K Mössbauer spectra of anaerobically purified pMMO recorded in parallel applied fields of 45 mT (A) and 8.0 T (B). The solid line in (A) is a spectral simulation for doublet 1, assigned to a diamagnetic diiron(III) center (20% of Fe), and a high-spin Fe^{2+} (18%) component. The remainder of the absorption (magnetic components) belongs to various high-spin Fe^{3+} species. The dashed line outlines doublet 1. The solid line in (B) is a spectral simulation for the putative diiron(III) center, assuming $S = 0$ and equivalent sites with $\Delta E_Q = +1.05$ mm/s, $\eta = 0.8$, and $\delta = 0.50$ mm/s; η is the asymmetry parameter of the electric field gradient tensor. The arrow points at the high-energy feature of the high-spin ferrous component. A second sample, exposed to oxygen after purification, gave identical spectra.

protein) when grown at high copper and iron concentrations, we were curious whether doublet 1 would be observed in whole cells. We have found that maximal pMMO activity in cell free fractions requires the addition of approximately $40 \mu\text{M}$ iron in conjunction with $80 \mu\text{M}$ copper in the culture media. We have recorded Mössbauer spectra of whole *M. capsulatus* Bath cells grown on media high in copper and iron between 1.5 and 120 K in applied fields up to 8.0 T. Figure 2B,D shows two representative 4.2 K spectra. The signal strength of the Mössbauer spectrum of Figure 2B indicates that the cells contain roughly 5 mM ^{57}Fe , in good agreement with the chemical analysis (5.2 mM). Approximately 40% of the iron belongs to a magnetic component of high-spin Fe^{3+} outlined by the solid line in (B); it yields a doublet with $\Delta E_Q \approx 0.6$ mm/s and $\delta = 0.45$ mm/s at 120 K (not shown). This component exhibits spectra typical of superparamagnetic nanoparticles,^{32,34} probably composed of mineralized excess iron accumulated during aerobic growth at high Fe concentrations. Simulation of the 45 mT spectrum of the superparamagnetic component of Figure 2B is quite straightforward (but not unique); however, fitting the outer four lines fixes position and intensities of the two innermost lines of the six-line pattern. Subtraction of the simulated superparamagnetic component from the raw data yields a spectrum (Figure 2C) which exhibits doublet 1 ($\sim 20\%$, solid line) with exactly the same parameters as observed in the purified enzyme. Also observed is a high-spin Fe^{2+} species with $\Delta E_Q \approx 3.00$ mm/s and $\delta \approx 1.25$ mm/s. The solid line in the 8.0 T spectrum of Figure 2D is a spectral simulation showing that the iron of doublet 1, as in the purified protein, belongs to a diamagnetic center. The broad features, stretching from ca. -9 to $+9$ mm/s Doppler velocity, belong to the superparamagnetic components³⁵ and the Fe^{2+} species. Finally, Figure 2A shows a 4.2 K Mössbauer spectrum of cells grown at low Cu and ^{57}Fe concentrations (each $5 \mu\text{M}$; pMMO $< 5\%$ of total cell protein) where pMMO expression is reduced 4-fold.⁶ Compared to the sample of Figure 2B, the signal amplitudes have declined by at least a factor 15, showing that the iron observed in the spectra of Figure 2B and D accumulates when the cells are growing at high Cu and Fe concentrations.

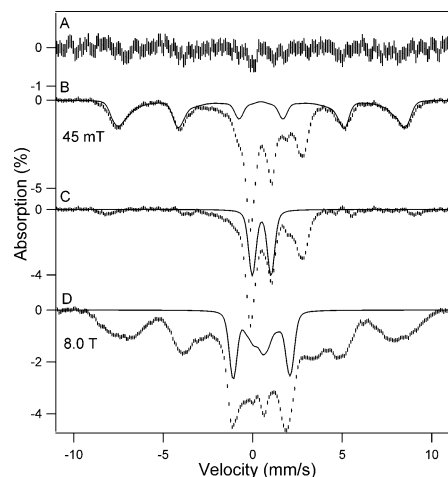


Figure 2. 4.2 K Mössbauer spectra of *M. capsulatus* Bath cells grown at $5 \mu\text{M}$ Cu and $5 \mu\text{M}$ ^{57}Fe (A) and at $80 \mu\text{M}$ Cu and $40 \mu\text{M}$ ^{57}Fe (B–D). The spectra were recorded in parallel applied fields as indicated. The sample of (B) and (D) consisted of cells grown at $80 \mu\text{M}$ Cu and $40 \mu\text{M}$ ^{57}Fe , then harvested, washed, and resuspended anaerobically. The solid line in (B), representing 40% of the ^{57}Fe , is a simulation of the superparamagnetic component, obtained by superimposing four high-spin ferric spectra; the simulation was solely aimed at representing the major fraction of the spectral area of this species at one particular applied field. (C) Difference spectrum obtained by subtracting the simulated spectrum of (B) from the raw data of (B). The solid line represents doublet 1 (20% of ^{57}Fe). (D) 8.0 T spectrum. The solid line is a simulation assuming that the iron of doublet 1 is diamagnetic.

The purified pMMO sample (1.06 mM $\alpha\beta\gamma$) had an iron concentration of 1.2 mM. If we associate the iron of doublet 1 with a diiron(III) cluster, we obtain a site occupancy of ca. 11%, assuming that pMMO can accommodate one diiron center/ $\alpha\beta\gamma$. The cells of Figure 2B had 5.2 mM iron, yielding $0.2 \times 5.2/2 = 0.52$ mM diiron centers. In previous experiments, we estimated that ca. 20% of the protein in cells cultured in media containing $80 \mu\text{M}$ Cu and $40 \mu\text{M}$ Fe belongs to pMMO.⁶ Using this estimate, the sample of Figure 2B has 0.56 mM pMMO, suggesting that pMMO in thus cultured cells has ~ 0.93 diiron(III) center/ $\alpha\beta\gamma$. The above estimates agree quite well with the observation that we recover ca. 10% of activity after purification of the protein.

We have assigned doublet 1 to a diiron(III) center. The Mössbauer properties of doublet 1 are also compatible with those observed for some low-spin ferrous hemes, such as cytochromes *c* and *b*, and $[\text{4Fe} - \text{4S}]^{2+}$ clusters. However, the UV/visible spectrum of the Mössbauer sample (Figure S2) indicates less than 0.005 hemes/ $\alpha\beta\gamma$, and the cellular concentration of heme in cells cultured in $5 \mu\text{M}$ Cu and $5 \mu\text{M}$ Fe is essentially identical to cells cultured in $80 \mu\text{M}$ Cu and $40 \mu\text{M}$ Fe.²⁰ $[\text{4Fe} - \text{4S}]^{2+}$ clusters can be excluded by observing that pMMO has only one cysteine residue, Cys 92 on the α subunit,^{21,36} and that the presence of sulfide has not been reported by any laboratory.

The Fe^{2+} components observed in whole cells have a larger ΔE_Q than the Fe^{2+} species observed in Figure 1A and thus represent a different type of Fe^{2+} , plausibly iron bound to transporters and storage components. Perhaps as much as 60% of the iron observed in the purified pMMO sample of Figure 1 belongs to high-spin Fe^{3+} . The EPR spectra of Figure S3 are almost devoid of iron-associated signals; the resonances at $g \approx 6$ and 4.3 account each for at most $10 \mu\text{M}$ Fe^{3+} , that is, only 1% of the iron. We suspect that the EPR-silent Fe^{3+} represents remnants of the mineralized fraction observed in whole cells that copurify with the enzyme. We have observed similar EPR-silent Fe^{3+} fractions in other proteins studied in our laboratory; invariably, these fractions disappeared as purification procedures improved. The reader may

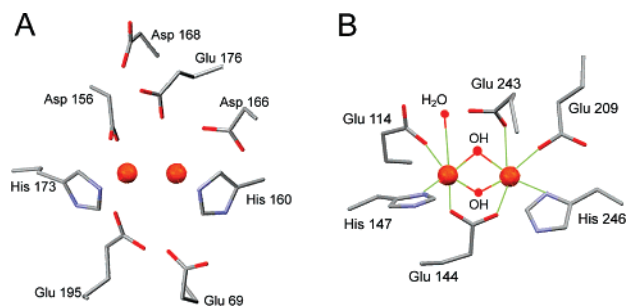


Figure 3. (A) Replacement of the mononuclear Zn by a diiron center in the X-ray structure of pMMO.²¹ (B) Environment of the diiron center in the sMMO from *M. trichosporium* OB3b.¹⁴

wonder whether doublet 1 could represent a dimer fraction of a mineralized Fe³⁺. We have recently studied Mössbauer spectra of *yah1-depleted* mitochondria from aerobically grown *S. cerevisiae*. For this mutant (which lacks iron–sulfur proteins), all detectable iron (2–3 mM) could be assigned to Fe³⁺ nanoparticles, with no evidence for a diamagnetic dimer fraction (unpublished results).

Given the similarities of the Mössbauer parameters of doublet 1 with those observed in sMMO, it is reasonable to propose that pMMO has an active site consisting of a diiron cluster, and that this cluster is bound in the site occupied by Zn from the crystallization buffer, a possibility indicated by Lieberman and Rosenzweig.²¹ Interestingly, this site has two conserved His and two conserved carboxylate residues (His160 and 173, Asp156, and Glu195). Moreover, the site has four additional nearby residues with carboxylate functions, Glu69, Glu176, Asp166, and Asp168, which are conserved in all known pMMO sequences. Thus, as shown in Figure 3A, the Zn site of pMMO has the requisite ligands to accommodate a sMMO-type diiron center and has suggestive similarities with the diiron site of sMMO, shown in Figure 3B. Placing the active site of pMMO into the Zn site is supported by the observation that exposure of the cells or purified pMMO to ¹⁴C-acetylene, a suicide substrate for pMMO, yields labeled β subunits (the copper sites of pMMO are located on α).^{20,37–39} With a target spectral signature, the loss of iron during purification of pMMO can now be studied by recording Mössbauer spectra through the various steps of the purification procedure.

Acknowledgment. This work was supported by the NIH Grant EB-001475 and Department of Energy Grant 96ER20237 and by the Office of Vice President for Research at The University of Michigan.

Supporting Information Available: UV–visible and EPR spectra, analytical data, and experimental details. This material is available free of charge via the Internet at <http://pubs.acs.org>.

References

- Anthony, C. *The Biochemistry of Methanotrophs*; Academic Press: London, 1982.
- Dalton, H. *Philos. Trans. R. Soc. London, Ser. B* **2005**, *360*, 1207–1222.
- Dalton, H.; Prior, S. D.; Leak, D. J.; Stanley, S. H. *Microbial Growth on C1 Compounds*; American Society for Microbiology, Washington, D.C., 1984; pp 75–82.
- Prior, S. D.; Dalton, H. *J. Gen. Microbiol.* **1985**, *131*, 155–163.
- Stanley, S. H.; Prior, S. D.; Leak, D. J.; Dalton, H. *Biotechnol. Lett.* **1983**, *5*, 487–492.
- Choi, D.-W.; Kunz, R. C.; Boyd, E. S.; Semrau, J. D.; Antholine, W. E.; Han, J. I.; Zahn, J. A.; Boyd, J. M.; de la Mora, A. M.; DiSpirito, A. A. *J. Bacteriol.* **2003**, *185*, 5755–5764.
- Murrell, J. C.; McDonald, I. R.; Gilbert, B. *Trends Microbiol.* **2000**, *8*, 221–225.
- Stolyar, S.; Franke, M.; Lidstrom, M. E. *J. Bacteriol.* **2001**, *183*, 1810–1812.
- Fox, B. G.; Froland, W. A.; Dege, J. E.; Lipscomb, J. D. *J. Biol. Chem.* **1989**, *264*, 10023–10033.
- Green, J.; Dalton, H. *J. Biol. Chem.* **1985**, *260*, 15795–15801.
- Waller, B. J.; Lipscomb, J. D. *Chem. Rev.* **1996**, *96*, 2625–2657.
- Waller, B. J.; Lipscomb, J. D. *Biochemistry* **2001**, *40*, 2220–2233.
- Fox, B. G.; Surerus, K. K.; Münck, E.; Lipscomb, J. D. *J. Biol. Chem.* **1988**, *263*, 10553–10556.
- Elango, W. A.; Radhakrishnan, R.; Froland, W. A.; Waller, B. J.; Earhart, C. A.; Lipscomb, J. D.; Olhendorf, D. H. *Protein Sci.* **1996**, *6*, 556–568.
- Liu, K. E.; Valentine, A. M.; Wang, A.; Huynh, B. H.; Edmondson, D. E.; Saligoglou, A.; Lippard, S. J. *J. Am. Chem. Soc.* **1995**, *117*, 10174–10185.
- Fox, B. G.; Hendrich, M. P.; Surerus, K. K.; Andersson, K. K.; Froland, W. A.; Lipscomb, J. D.; Münck, E. *J. Am. Chem. Soc.* **1993**, *115*, 3688–3701.
- Basu, P.; Katterle, B.; Andersson, K. K.; Dalton, H. *Biochem. J.* **2003**, *369*, 417–427.
- Lieberman, R. L.; Shrestha, D. B.; Doan, P. E.; Hoffman, B. M.; Stemmler, T. L.; Rosenzweig, A. C. *Proc. Natl. Acad. Sci. U.S.A.* **2003**, *100*, 3820–3825.
- Takeguchi, M.; Miyakawa, K.; Okura, I. *J. Mol. Catal. A* **1998**, *132*, 145–153.
- Zahn, J. A.; DiSpirito, A. A. *J. Bacteriol.* **1996**, *178*, 1018–1029.
- Lieberman, R. L.; Rosenzweig, A. C. *Nature* **2005**, *434*, 177–182.
- Nguyen, H. H.; Elliott, S. J.; Yip, J. H.; Chan, S. I. *J. Biol. Chem.* **1998**, *273*, 7957–7966.
- Hakemian, A. S.; Rosenzweig, A. C. *Annu. Rev. Biochem.* **2007**, *76*, 223–241.
- Chan, S. I.; Chen, K. H.-C.; Yu, S. S.-F.; Chen, C. L.; Kuo, S. S. J. *Biochemistry* **2004**, *43*, 4421–4430.
- Chan, S. I.; Wang, V. C.-C.; Lai, J. C.-H.; Yu, S. S.-F.; Chen, P. P.-Y.; Chen, K. H.-C.; Chen, C.-L.; Chan, M. K. *Angew. Chem., Int. Ed.* **2007**, *46*, 1992–1994.
- Choi, D. W.; Antholine, W. E.; Do, Y. S.; Semrau, J. D.; Kisting, C. J.; Kunz, R. C.; Campbell, D.; Rao, V.; Hartsel, S. C.; DiSpirito, A. A. *Microbiology* **2005**, *151*, 3417–3426.
- Myronova, N.; Kitmitto, A.; Collins, R. F.; Miyajiri, A.; Dalton, H. *Biochemistry* **2006**, *45*, 11905–11914.
- Takeguchi, M.; Ohashi, M.; Okura, I. *BioMetals* **1999**, *12*, 123–129.
- Tukhvatullin, I. A.; Gvozdev, R. I.; Andersson, K. K. *Biochem. Biophys. Mol. Biol.* **2000**, *374*, 177–182.
- Lieberman, R. L.; Kondapalli, K. C.; Shrestha, D. B.; Hakemian, A. S.; Smith, S. M.; Telsler, J.; Kuzelka, J.; Gupta, R.; Borovik, A. S.; Lippard, S. J.; Hoffman, B. M.; Rosenzweig, A. C.; Stemmler, T. L. *Inorg. Chem.* **2006**, *45*, 8372–8381.
- DeWitt, J. G.; Bentsen, J. G.; Rosenzweig, A. C.; Hedman, B.; Green, J.; Pilkington, S.; Papaefthymiou, G. C.; Dalton, H.; Hodgson, K. O.; Lippard, S. J. *J. Am. Chem. Soc.* **1991**, *113*, 9219–9235.
- Lesuisse, E.; Santos, R.; Matzkanke, B. F.; Knight, S. A. B.; Camadro, J.-M.; Dancis, A. *Hum. Mol. Genet.* **2003**, *12*, 879–889.
- Vrajmasu, V. V.; Bominaar, E. L.; Meyer, J.; Münck, E. *Inorg. Chem.* **2002**, *41*, 6358–6371.
- Long, G. L. *Mössbauer Spectroscopy Applied to Inorganic Chemistry*; Plenum Press: New York, 1984; Vol. 2.
- The magnetic spectra of superparamagnetic particles are exceedingly complex as they depend on the size, shape, and shape distribution of these particles; see ref 34.
- Semrau, J. D.; Chistoserdov, A.; Lebron, J.; Costello, A.; Davagnino, J.; Kenna, E.; Holmes, A. J.; Finch, R.; Murrell, J. C.; Lidstrom, M. E. *J. Bacteriol.* **1995**, *177*, 3071–1379.
- DiSpirito, A. A.; Gullledge, J.; Shiemke, A. K.; Murrell, J. C.; Lidstrom, M. E.; Crema, C. L. *Biodegradation* **1992**, *2*, 151–164.
- Hyman, M.; Arp, D. J. *J. Biol. Chem.* **1992**, *267*, 1534–1545.
- Prior, S. D.; Dalton, H. *FEMS Microbiol. Lett.* **1985**, *29*, 105–109.

JA077682B